Published in final edited form as:
*Biochemistry*. 2011 October 11; 50(40): 8540–8547. doi:10.1021/bi200710m.

# Effects of a Protecting Osmolyte on The Ion Atmosphere Surrounding DNA Duplexes

**Joshua M. Blose**, **Suzette A. Pabit**, **Steve P. Meisburger**, **Li Li**, **Christopher D. Jones**, and **Lois Pollack***
School of Applied and Engineering Physics, Cornell University, Ithaca, New York 14853, United States

## Abstract

Osmolytes are small, chemically diverse, organic solutes that function as an essential component of cellular stress response. Protecting osmolytes enhance protein stability via preferential exclusion, and non-protecting osmolytes, such as urea, destabilize protein structures. Although much is known about osmolyte effects on proteins, less is understood about osmolyte effects on nucleic acids and their counterion atmospheres. Non-protecting osmolytes destabilize nucleic acid structures, but effects of protecting osmolytes depend on numerous factors including the type of nucleic acid and the complexity of the functional fold. To begin quantifying protecting osmolyte effects on nucleic acid interactions we used small angle x-ray scattering (SAXS) techniques to monitor DNA duplexes in the presence of sucrose. This protecting osmolyte is a commonly used contrast matching agent in SAXS studies of protein-nucleic acid complexes, thus it is important to characterize interaction changes induced by sucrose. Measurements of interactions between duplexes showed no dependence on the presence of up to 30% sucrose except under high $Mg^{2+}$ conditions where stacking interactions were disfavored. The number of excess ions associated with DNA duplexes, reported by anomalous small angle x-ray scattering (ASAXS) experiments, was sucrose independent. Although protecting osmolytes can destabilize secondary structures, our results suggest that ion atmospheres of individual duplexes remain unperturbed by sucrose.

Osmolytes are small intracellular organic solutes that function as a vital component of cellular stress response.[1–4] They are chemically diverse and include polyols, sugars, amino acids, and methylamines. Organisms preferentially utilize subsets of these molecules.[1, 3–4] For example, under conditions of increased salinity, plants accumulate a variety of osmolytes such as amino acids (proline and valine) and sugars (glucose and sucrose), however, *Saccharomyces cerevisae* utilizes glycerol as an osmolyte in a near-exclusive fashion.[4] Despite these differences in chemical structure and stress-specificity, protecting or compatible osmolytes enhance protein stability by the same chemical mechanism: preferential exclusion.[2, 5–6] The protecting osmolyte is excluded from the surface of the protein, making denaturation less energetically favorable than in an aqueous environment. Thus, the ratios of protecting to non-protecting osmolytes as well as protecting osmolytes to ions must be carefully maintained to preserve protein structure and protein-nucleic acid interactions.[7–9]

In contrast to osmolyte effects on protein stability, structure, and function, the effects of osmolytes on nucleic acids are generally less well understood. Non-protecting osmolytes such as urea can destabilize nucleic acid structures and are commonly utilized in folding

*Tel: (607) 255-8695; Fax: (607) 255-7658; lp26@cornell.edu.

**Supporting Information Available**: Plots of Relative Fluorescence of HQS-$Mg^{2+}$ complex with increasing $Mg^{2+}$ in 0 and 30% sucrose. This material is available free of charge via the Internet at http://pubs.acs.org.

studies.[10–16] However, the effects of protecting osmolytes on nucleic acid structure depend on the type of nucleic acid, its structural complexity, and folding interactions. Although most protecting osmolytes destabilize secondary structure, their effects on tertiary or higher order structure formation rely on various complex interactions. Changes in nucleic acid hydration and nucleic acid-osmolyte interactions must be balanced against the impact of molecular crowding and changes in excluded volume.[17–30] Moreover, the effects of osmolytes on ion atmospheres of nucleic acids have not been fully characterized. The complementary or sometimes opposing effects of ions and osmolytes as well as attenuation of osmolyte-$Mg^{2+}$ stabilization of nucleic acid structure are beginning to be studied[21, 27], but important structural properties such as the number of bound ions have so far been determined by indirect measurement.[23] Here we describe results of experiments designed to probe the effects of osmolytes on nucleic acid electrostatics and the ion atmosphere. We examined the interactions of a 25 base pair (bp) DNA duplex in the presence and absence of sucrose, a protecting osmolyte, using small angle x-ray scattering (SAXS) techniques. Sucrose is an important contrast matching agent in SAXS studies of protein-nucleic acid complexes. At elevated concentrations, sucrose's electron density matches that of protein, rendering it (mostly) indistinguishable from the solvent. Nucleic acids have higher electron densities than proteins, so are not contrast matched even at these increased sucrose concentrations. Contrast matching studies have been used to selectively probe the nucleic acid portion of complexes including the ribosome and nucleosome core particles.[31–34] Although sucrose can destabilize nucleic acid secondary structures[21–22], we find that electrostatic interactions between duplexes remained unaffected even in 30% sucrose except under high salt conditions where the duplexes can interact via intermolecular stacking. In addition, anomalous small angle x-ray scattering (ASAXS) experiments report no change in the number of ions around the duplexes as the sucrose content of the solution increases from 0% to 30%. The shape of the anomalous scattering signal reports the ion correlation to the nucleic acid, and it is not modified by added sucrose, suggesting that the spatial distribution of the ions is unaffected by the presence of this osmolyte. Taken together, these results suggest that both electrostatic interactions between duplexes and the ion atmospheres around individual duplexes remain unperturbed by sucrose. Moreover, this approach is easily extended to elucidate the role of other osmolytes in modifying nucleic acid interactions.

## Materials and Methods

### DNA Duplex Preparation

The desalted and purified single-strand components of the 25 bp DNA were purchased from Integrated DNA Technologies (IDT, Coralville, IA). The DNA sequence GCATCTGGGCTATAAAAGGGCGTCG, is the same as in previous studies.[35–39] Lyophilized samples were reconstituted in an annealing buffer of 10 millimolal (m*m*) TRIS, 1 m*m* EDTA, and 50 m*m* NaCl at pH 8.0. Concentrations of the single-strands were calculated using UV absorbance at 260 nm, and equimolar amounts of the complementary strands were mixed and annealed at 95°C for two minutes before the solutions were allowed to slowly cool to room temperature. For SAXS experiments, the duplex strands were then dialyzed extensively against bulk 1 m*m* $Na^+$ MOPS solutions (pH 7) containing $MgCl_2$ using Amicon Ultra centrifugal filter units (Millipore Corporation, Billerica, MA) with a 10,000 nominal molecular weight limit. Sucrose was added to samples post-dialysis for 0.32 and 1.25 *m* concentrations which we report as the more familiar 10 and 30% (wt.%), respectively. DNA duplexes were prepared for final concentrations of approximately 0.15 and 0.5 m*m* duplex for “low” and “high” concentration samples, respectively. The concentrations were determined from absorbance at 260 nm, and the duplex extinction coefficient was calculated from extinction coefficients of the single strands as previously described.[40] DNA duplex samples for ASAXS measurements were prepared in similar

fashion to those used for SAXS, except that these samples were dialyzed against 1 m*m* $Na^+$ MOPS solutions (pH 7) containing either rubidium acetate ($Rb^+$ acetate) for ASAXS samples or sodium acetate ($Na^+$ acetate) for the control samples. Rb is used for ASAXS experiments because of its readily accessible absorption edge near 15 keV. The energy of the comparable edge for Na is inaccessible.

## SAXS Experiments and Determination of Second Virial Coefficients

All SAXS and ASAXS experiments were performed at the Cornell High Energy Synchrotron Source (CHESS) C1 station. SAXS profiles effectively report on interactions between DNA duplexes in solution.[35–36, 38, 41] The concentration normalized scattering intensity *I(q)* is given by Equation 1.

$$I(q) = P(q)\, S(c,q). \quad (1)$$

Here, *c* is the concentration of molecules, and *q* is the momentum transfer $(4\pi/\lambda)*\sin\theta$, where $\lambda$ is the x-ray wavelength, and $2\theta$ is the scattering angle. *P(q)* (form factor) is the spherically averaged scattering from an individual molecule, and *S(c,q)* (effective structure factor) is related to the spatial arrangement of the molecules: *S(c,q)* describes intermolecular interactions and accounts for short range order in the ensemble. This effective structure factor relies on a spherical approximation, which is valid for short duplexes.[41] The second virial coefficient ($A_2$), provides a measure of intermolecular interaction potential and can be derived from a linear fit to the following expression[35–36, 38, 41]:

$$\frac{1}{S(c,q=0)} = 1 + 2MA_2c. \quad (2)$$

In equation 2, *S(c,q=0)* is the effective structure factor extrapolated to *q = 0*, M is the molecular weight of the molecule, and *q* and *c* are the same as in equation 1. To use equation 2, *P(q)* must be known either from experiment or calculation.[35–36, 38, 41] However, the following expression is obtained by substituting the reciprocal of equation 1 into equation 2:

$$\frac{1}{I(q=0)} = \frac{2MA_2c}{P(q=0)} + \frac{1}{P(q=0)}. \quad (3)$$

This equation defines a strategy for finding $A_2$ without knowledge of *P(q)*: divide the slope ($2MA_2/P(q=0)$) by the intercept ($1/P(q=0)$). This approach is useful when accurate measurements of *P(q)* may be difficult to obtain experimentally due to high scattering of the osmolyte in solution, or subtle osmolyte-induced contrast variation effects in multicomponent systems. Reference 41 outlines a detailed procedure for extracting $A_2$ from SAXS data.

## ASAXS Experiments and Counting Ions around DNA Duplexes

ASAXS experiments, which exploit the energy dependence of scattering factors of ions around the DNA duplex, were performed to measure the spatial distribution of associated monovalent cations (100 m*m* $Rb^+$ acetate, 100 m*m* $Na^+$ acetate controls). Both the number and distributions of ions surrounding the 25 bp DNA duplex were obtained in the presence of 0, 10, and 30% sucrose. The ASAXS technique was recently reviewed, and important experimental details were described including the beamline set-up, background subtraction, and fluorescence correction.[37–38, 41–42] In addition, absolute calibration of the ASAXS signals enables measurement of the number of excess ions in solution due to the presence of the nucleic acid ($N_{ions}$).[39] Excess ions are the charge-compensating ions present in the

DNA-containing solution, relative to the bulk solvent. The number of excess ions is easily computed using scattering profiles measured at two x-ray energies[39]:

$$N_{ions} = \sqrt{\frac{\alpha}{S\,(c, q=0)}} \frac{\sqrt{I\,(q=0, E_1)} - \sqrt{I\,(q=0, E_2)}}{f'\,(E_1) - f'\,(E_2)} \quad (4)$$

In equation 4, *I(q=0)* is the concentration normalized scattering intensity extrapolated to $q = 0$, and *S(c,q=0)* is as in equation 1. Alpha (α), the scale factor for absolute intensity calibration, is determined using the procedure discussed in reference 37. $E_1$ and $E_2$ are x-ray energies 1 and 2 and the $f'$ are (sucrose-independent) ion scattering factors at x-ray energies 1 and 2 respectively. For these experiments, $E_1$ = 15.093 keV, $E_2$ = 15.193 keV, $f'(E_1)$ = −4.09, and $f'(E_2)$ = −7.02 electrons.

### UV Melting Experiments

DNA duplex melt samples were prepared by diluting aliquots of the SAXS samples to approximately 5 μ*m* duplex with the same buffers and sucrose solutions as used in the SAXS experiments. Due to the high stability of duplexes in 100 m*m* $MgCl_2$ melts were not possible. UV melts used a Cary 50 UV-Vis spectrophotometer (Varian Inc., Australia) with a data point acquired every 0.5 °C at a wavelength of 260 nm. The DNA was thermally denatured and refolded over temperature ranges of 15 to 95 °C and 95 to 15 °C. The rate of temperature changes was 1 °C/minute and provided data consistent with reversibility of the two-state folding transition. Absorbance curves were fit to determine thermodynamic parameters using *MeltWin 3.5* software.[43]

## Results and Discussion

### Sucrose Does Not Affect Inter-Duplex Interactions Except at High $Mg^{2+}$ Concentrations

Past studies of this 25 bp duplex[35–36, 38] have quantified the interactions of monovalent and divalent cations with DNA, as well as ion-induced interactions between DNA. Here, we address changes in inter-duplex interactions following variation of a third parameter: sucrose concentrations between 0 and 30%. To enable comparison with past studies, $Rb^+$ acetate was selected as the monovalent salt. Importantly, $Rb^+$ is the lightest monovalent counterion compatible with ASAXS. Studies were carried out at both 50 and 100 m*m* $Rb^+$ acetate, where repulsive interactions between duplexes dominate. SAXS studies on divalent ions were restricted to $MgCl_2$ at concentrations of 3 and 100 m*m* $MgCl_2$. In 0% sucrose, repulsive interactions between DNAs are measured at low $Mg^+$ concentrations and end-to-end stacking of helices is observed at higher $Mg^+$ concentrations.[35–36, 38, 44] A discussion of the uniqueness of this interpretation can be found in the supplemental information for reference 38. Lastly, the DNA samples were prepared at two different concentrations, approximately 0.15 m*m* and 0.5 m*m* duplex respectively, to probe interparticle interactions and enable application of Equations 2 or 3.[35–36, 38]

Concentration normalized SAXS scattering profiles for DNA in $Rb^+$ are shown in Figure 1. Panels A–C of Figure 1 show Rb-DNA in the presence of 0, 10, and 30% sucrose. At 0% sucrose (Figure 1A) trends are identical to those reported previously.[35–36, 38] For a given concentration of $Rb^+$ acetate (e.g. 50 mm $Rb^+$) increasing DNA concentration (blue to orange curves) causes a decrease in intensity at low $q$, $q < 0.05$, consistent with greater repulsion between helices and increased variation of *S(c,q)*. Additionally, scattering profiles acquired at a fixed DNA concentration display more repulsion at lower ionic strength, e.g. the low $q$ scattering profile is further depressed in 50 m*m* compared with 100 m*m* $Rb^+$. This effect becomes more pronounced at higher DNA concentration, e.g. compare the orange and green curves in Figure 1A. As the sucrose concentration increases to 10% (Figure 1B) then

to 30% (Figure 1C), the overall signal strength drops due to the decreasing contrast with electron dense sucrose. Despite this overall decrease, the trends observed at 0% sucrose persist: the enhancement of repulsive forces resulting from a decrease in salt concentration and/or an increase in DNA concentrations is manifested as a decrease in the low $q$ scattering intensity. Qualitatively, the data of Figure 1 suggest that sucrose neither enhances nor disrupts inter-duplex interactions in monovalent salt.

Sucrose dependent SAXS scattering profiles for the 25 bp DNA duplex in the presence of $MgCl_2$ are shown in Figure 2. In the absence of sucrose, these data agree with previous measurements: at 3m$m$ $Mg^{2+}$ data (blue and orange curves), increasing DNA concentration results in a decrease in scattering intensity at low $q$, reflecting greater repulsion between duplexes.[35–36, 38] In contrast, when solutions contain 100 mm $Mg^{2+}$ (red and green curves), an increase in DNA concentration results in increased low $q$ intensity, consistent with the stacking of DNA duplexes into extended helical structures.[35–36, 38, 44] This ionic strength dependence follows previously established trends: repulsion is enhanced as ionic strength decreases. As a function of increasing sucrose (Figure 2A–C) the intensity of each curve decreases due to the contrast matching effects of the osmolyte, as observed in the $Rb^+$ data (Figure 1A–C). However, whereas the inter-DNA repulsion measured at 3 m$m$ $Mg^{2+}$ persists at all sucrose concentrations (orange and blue curves, all panels Figure 2), $Mg^{2+}$-induced association of helices depends on sucrose. The enhanced scattering intensity at low $q$ with increasing DNA concentration, indicative of end-to-end stacking of duplexes, vanishes at 30% sucrose (Figure 2C). There is a measurable decrease in the population of end-to-end stacked duplexes. Thus, the data of Figure 2 suggest that addition of sucrose does not modify the repulsive forces present at low concentrations of divalent salts, but sucrose hinders formation of superstructure in the presence of high concentration of divalent salt.

To quantify the strength of the repulsive interactions, we computed the second virial coefficient, $A_2$ for both the $Rb^+$ and $Mg^{2+}$ containing samples (Figure 3). In general, $A_2 > 0$ signifies net repulsion and $A_2 < 0$ (Figure 3, shaded region) implies net attraction between biomolecules. For both 50 m$m$ and 100 m$m$ $Rb^+$ $A_2$ is positive. In accord with measurements at 0% sucrose, the $A_2$ values are larger at 50 m$m$ than 100 m$m$ $Rb^+$. Moreover, the $A_2$ values for 0, 10, and 30% sucrose samples (circle, square, and triangle, respectively) are the same within error for a given $Rb^+$ concentration. Thus the $A_2$ data demonstrate that duplex interactions in monovalent salt are unperturbed by added sucrose.

Unlike the $Rb^+$ data, the $A_2$ values for the $Mg^{2+}$ containing samples show different trends with increasing sucrose depending on the $Mg^{2+}$ concentration. At 0% sucrose, $A_2$ is consistent with previously published values.[38] In the presence of 3 m$m$ $Mg^{2+}$, $A_2$ is positive, and as with the monovalent ion data, independent of sucrose concentration up to 30%. In contrast, in 100 m$m$ $Mg^{2+}$, the magnitude of $A_2$ decreases with added sucrose, reflecting weaker interparticle association. This perturbation of inter-duplex interactions suggests interplay between the osmolyte and the helical stacking.

In summary, the scattering profiles and $A_2$ values measured as a function of sucrose suggest that the osmolyte does not affect inter-duplex interactions in the presence of monovalent and low concentrations of divalent counterions where only secondary structure is present. However, in presence of high concentrations of divalent counterions, sucrose disrupts the formation of higher order structure.

## Sucrose Does Not Change the Distribution or Number of Ions around DNA Duplexes

To probe the ion atmosphere of the 25 bp DNA, ASAXS was used to count the number of excess ions around the duplex in the presence of 0, 10, and 30% sucrose. ASAXS scattering profiles are sensitive to counterion-DNA distances[42], thus also provide the spatial

correlation of these ions to the duplex. The anomalous scattering profiles for both the 100 m*m* $Rb^+$ acetate samples and the 100 m*m* $Na^+$ acetate controls are shown in Figure 4A. As expected, the controls show near zero scattering intensity. Since no resonant elements are present, no variation of scattering with energy is expected for these samples. As sucrose is added, the overall size of the anomalous signal decreases, which reflects the changing contrast. However, the shape of the anomalous scattering profile is sucrose independent. Thus, the quantity of interest, e.g. the spatial distribution of ions around the DNA, does not change with sucrose. Figure 4B displays the data on a logarithmic scale and highlights the similar shape of these profiles. From these data we conclude that sucrose does not alter the distribution of ions around the duplex.[38]

The number of excess ions around the duplex was calculated using Equation 4 (Materials and Methods), and $N_{ions}$ is shown in Figure 5. In 0% sucrose $N_{ions}$ equals 34 ± 3, in good agreement with previous counting experiments and NLPB calculations.[39] This value remains constant (within error) with increasing sucrose, reinforcing the conclusions drawn from the SAXS data: electrostatic interactions are minimally dependent on sucrose concentration. Thus, both the distribution and number of monovalent ions around DNA appears independent of sucrose; sucrose does not perturb nucleic acid ion atmospheres in monovalent salt background.

## Sucrose Destabilizes DNA Duplexes

The SAXS and ASAXS data presented above suggest that sucrose does not alter inter-duplex interactions or the duplex ion atmosphere in 50 and 100 m*m* $Rb^+$ acetate or in 3 m*m* $MgCl_2$. To determine any other effects of sucrose on duplex structure, we examined duplex stability via UV melts of SAXS samples for these three ionic conditions in 0 and 30% sucrose. Thermal denaturation of the 100 m*m* $Mg^{2+}$ sample was not attempted due to the high stability of the duplex. Typical melting curves are shown in Figure 6; the thermodynamic parameters extracted from analysis of the curves are provided in Table 1. For all ionic conditions studied, the duplex was destabilized by sucrose, consistent with reports that sucrose destabilizes other nucleic secondary structures.[21–22] The destabilization was larger for samples containing monovalent ions, and compares well in magnitude with previous measurements of similarly sized polyethylene glycols and comparable length DNA duplexes.[19] Although the observed change in folding free energy with increasing sucrose is significant, all x-ray scattering experiments were conducted at room temperature (~25° C) well below the melting temperatures ($T_M$) for the observed unfolding transitions. Thus, although sucrose does destabilize the duplex as suggested from osmolyte literature, it does not significantly affect the folded populations in our scattering experiments.

## End-to-End Interhelical Stacking is Destabilized by Sucrose

DNA duplex interactions as well as the number and distribution of ions around the duplex remained unaltered under most experimental conditions, yet in the presence of 100 m*m* $MgCl_2$, sucrose modifies interparticle interactions (the magnitude of $A_2$ decreases). To reconcile these observations we proposed an interaction scheme (Figure 7) similar to a model for general osmolyte effects previously presented to describe folding of RNA secondary and tertiary structures.[21] For the purposes of this model no sucrose-induced changes to the ion atmosphere are considered, consistent with the ASAXS characterization presented above. In addition, we do not consider changes in excluded volume commonly associated with the molecular crowding phenomena. Excluded volume effects can be significant to the stabilization and function of nucleic acids[26] and large molecular weight crowding agents have been shown to stabilize duplexes[17, 19, 22, 30]. However, the destabilization of secondary structure in the presence of smaller cosolutes such as most osmolytes[17, 19–23, 30], and the sucrose destabilization of the 25 bp DNA duplex herein is

opposite the stabilization observed when excluded volume effects are dominant. Therefore, excluded volume effects are unlikely to play a significant role in explaining our experimental results. The proposed interaction scheme does not include changes in ion activity due to the presence of sucrose. Thirty-percent sucrose can increase the activity coefficient of 100 m*m* NaCl from 0.778[45] to 0.799[46], which is measurable but small, and it is unlikely that $Rb^+$-sucrose interactions are substantially larger than those for $Na^+$-sucrose. These small changes are below the sensitivity of the ASAXS data. In contrast, there is a paucity of literature concerning the effects of sucrose on divalent ion activity. However, we used 8-hydroxyquinoline-5-sulfonic acid, a dye that reports $Mg^{2+}$ activity in RNA studies[47], to measure $Mg^{2+}$ activity in sucrose-containing solutions. Binding curves of the $Mg^{2+}$ - HQS complex in 0% and 30% sucrose are nearly identical, suggesting that the presence of sucrose does not greatly impact $Mg^{2+}$ activity (Figure S1). Since the measured changes in $A_2$ observed in 30% sucrose would require an ~10× change in $Mg^{2+}$ activity, we conclude that the effects of sucrose on $Mg^{2+}$ activity are small compared to its effects on end-to-end stacking.

Within the constraints described above, the interaction scheme of Figure 7 summarizes our observations. In the single-stranded state the bases are solvent exposed, and sucrose accumulates around the bases (first panel). This condition applies to all experimental conditions. When the single strands fold to form the duplex (second panel), bases become buried in the helix via stacking and inaccessible to sucrose. This step is consistent with thermodynamic studies on DNA folding and sucrose which suggest significant changes in water and sucrose organization as well as inaccessibility of sucrose to interior base pairs formed in duplex hybridization.[17, 19, 22]

In high concentrations of $Mg^{2+}$, efficient charge screening of the duplex by divalent ions allows for end-to-end stacking, shown in the second transition in Figure 7. This stacking is disrupted when sucrose is added. This effect can be understood by accounting for the preferential interaction of sucrose with the non-stacked bases at the ends of the helix. In contrast to the bases within the interior of the duplex, osmolyte can accumulate around these solvent-exposed ends. Duplex stacking requires release of this included sucrose to the solvent (yellow molecules in panel). Thus, end-to-end stacking is disfavored at 30% sucrose relative to 0% sucrose, reflected by a decrease in the magnitude of $A_2$. This destabilization of super secondary structure differs from the stabilizing effect of other osmolytes such as trimethylamine, which is excluded from phosphate groups and stabilizes structures which bury the nucleic acid backbone.[27] These differences in osmolyte-nucleic acid interactions suggest that the identity, concentration, and ratios of osmolytes, as well as the types of surface area buried in forming super secondary and folding tertiary structures all play critical roles in determining the stability and population of functional nucleic acids as cells react to stresses and adapt to changing cellular environments.

## Conclusion

As interest in the role of osmolytes in cellular processes continues to expand, it is critically important to understand the physiochemical mechanisms of their effects on the structure and stability of functional nucleic acids. Experiments described here employed both SAXS and ASAXS to monitor ion-DNA as well as inter-DNA interactions as a function of increasing sucrose concentration. The presence of even large concentrations of sucrose does not perturb electrostatic interactions when monovalent ions or low concentrations of divalent cations are present in the buffer. The number of excess ions remains constant, as does the second virial coefficient reporting interduplex interactions. Sucrose induced changes were observed only when divalent cations were present at concentrations that enabled end-to-end stacking of duplexes. We propose that sucrose alters these interactions by disfavoring interhelical

stacking. To describe these results we invoke an interaction scheme that considers the burial of base surfaces from sucrose upon folding or stacking of the duplexes. Thus, inclusion of sucrose by DNA bases is a model for osmolyte effects on the DNA duplexes. This model of inclusion and solvation is similar in principle to that proposed for osmolyte-protein interactions. We note that protecting osmolytes may destabilize or stabilize nucleic acid structures depending on the types of moieties (phosphate backbone vs. bases) exposed or made inaccessible during folding transitions, and for smaller cosolutes such as sucrose, preferential interactions are likely to dominate the nucleic acid interactions rather than excluded volume effects or changes to counterion atmopshere. Therefore, our observations suggest that sucrose's use as a contrast matching agent in SAXS experiments does not alter ion atmosphere around short DNA duplexes and underscores the utility of ASAXS as a probe of osmolyte effects on nucleic acid interactions.

## Supplementary Material

Refer to Web version on PubMed Central for supplementary material.

## Acknowledgments

We thank Ken Finkelstein for his experimental assistance at the Cornell High Energy Synchrotron Source (CHESS).

Funding: Funding for this research was provided by NIH grants: GM-088645, GM-085062 and T32 GM-008267. Additional support was provided by the Cornell Nanobiotechnology Center. CHESS is supported by the NSF & NIH/NIGMS via NSF award DMR-0936384.

## Abbreviations

| | |
|---|---|
| **(ASAXS)** | anomalous small angle x-ray scattering |
| **(bp)** | base pair |
| **(MOPS)** | 3 - (N - morpholino) propanesulfonic acid |
| **(SAXS)** | small angle x-ray scattering |
| **$T_M$** | melting temperature |

## References

1. Yancey PH, Clark ME, Hand SC, Bowlus RD, Somero GN. Living with water stress: evolution of osmolyte systems. Science. 1982; 217:1214–1222. [PubMed: 7112124]
2. Bolen DW. Protein stabilization by naturally occurring osmolytes. Methods Mol Biol. 2001; 168:17–36. [PubMed: 11357625]
3. Yancey PH. Organic osmolytes as compatible, metabolic and counteracting cytoprotectants in high osmolarity and other stresses. J Exp Biol. 2005; 208:2819–2830. [PubMed: 16043587]
4. Burg MB, Ferraris JD. Intracellular organic osmolytes: function and regulation. J Biol Chem. 2008; 283:7309–7313. [PubMed: 18256030]
5. Timasheff SN. The control of protein stability and association by weak interactions with water: how do solvents affect these processes? Annu Rev Biophys Biomol Struct. 1993; 22:67–97. [PubMed: 8347999]
6. Auton M, Bolen DW, Rosgen J. Structural thermodynamics of protein preferential solvation: osmolyte solvation of proteins, aminoacids, and peptides. Proteins. 2008; 73:802–813. [PubMed: 18498104]
7. Lin TY, Timasheff SN. Why do some organisms use a urea-methylamine mixture as osmolyte? Thermodynamic compensation of urea and trimethylamine N-oxide interactions with protein. Biochemistry. 1994; 33:12695–12701. [PubMed: 7918496]

8. Wang A, Bolen DW. A naturally occurring protective system in urea-rich cells: mechanism of osmolyte protection of proteins against urea denaturation. Biochemistry. 1997; 36:9101–9108. [PubMed: 9230042]

9. Record MT Jr. Courtenay ES, Cayley S, Guttman HJ. Biophysical compensation mechanisms buffering E. coli protein-nucleic acid interactions against changing environments. Trends Biochem Sci. 1998; 23:190–194. [PubMed: 9612084]

10. Pan T, Sosnick TR. Intermediates and kinetic traps in the folding of a large ribozyme revealed by circular dichroism and UV absorbance spectroscopies and catalytic activity. Nat Struct Biol. 1997; 4:931–938. [PubMed: 9360610]

11. Rook MS, Treiber DK, Williamson JR. Fast folding mutants of the Tetrahymena group I ribozyme reveal a rugged folding energy landscape. J Mol Biol. 1998; 281:609–620. [PubMed: 9710534]

12. Shelton VM, Sosnick TR, Pan T. Applicability of urea in the thermodynamic analysis of secondary and tertiary RNA folding. Biochemistry. 1999; 38:16831–16839. [PubMed: 10606516]

13. Sosnick TR. Characterization of tertiary folding of RNA by circular dichroism and urea. Curr Protoc Nucleic Acid Chem Chapter. 2001; 11 Unit 11 15.

14. Brown TS, Chadalavada DM, Bevilacqua PC. Design of a highly reactive HDV ribozyme sequence uncovers facilitation of RNA folding by alternative pairings and physiological ionic strength. J Mol Biol. 2004; 341:695–712. [PubMed: 15288780]

15. Russell R, Das R, Suh H, Travers KJ, Laederach A, Engelhardt MA, Herschlag D. The paradoxical behavior of a highly structured misfolded intermediate in RNA folding. J Mol Biol. 2006; 363:531–544. [PubMed: 16963081]

16. Priyakumar UD, Hyeon C, Thirumalai D, Mackerell AD Jr. Urea destabilizes RNA by forming stacking interactions and multiple hydrogen bonds with nucleic acid bases. J Am Chem Soc. 2009; 131:17759–17761. [PubMed: 19919063]

17. Spink CH, Chaires JB. Effects of hydration, ion release, and excluded volume on the melting of triplex and duplex DNA. Biochemistry. 1999; 38:496–508. [PubMed: 9890933]

18. Gluick TC, Yadav S. Trimethylamine N-oxide stabilizes RNA tertiary structure and attenuates the denaturating effects of urea. J Am Chem Soc. 2003; 125:4418–4419. [PubMed: 12683801]

19. Nakano S, Karimata H, Ohmichi T, Kawakami J, Sugimoto N. The effect of molecular crowding with nucleotide length and cosolute structure on DNA duplex stability. J Am Chem Soc. 2004; 126:14330–14331. [PubMed: 15521733]

20. Hong J, Capp MW, Saecker RM, Record MT Jr. Use of urea and glycine betaine to quantify coupled folding and probe the burial of DNA phosphates in lac repressor-lac operator binding. Biochemistry. 2005; 44:16896–16911. [PubMed: 16363803]

21. Lambert D, Draper DE. Effects of osmolytes on RNA secondary and tertiary structure stabilities and RNA-Mg2+ interactions. J Mol Biol. 2007; 370:993–1005. [PubMed: 17555763]

22. Spink CH, Garbett N, Chaires JB. Enthalpies of DNA melting in the presence of osmolytes. Biophys Chem. 2007; 126:176–185. [PubMed: 16920250]

23. Nakano S, Wu L, Oka H, Karimata HT, Kirihata T, Sato Y, Fujii S, Sakai H, Kuwahara M, Sawai H, Sugimoto N. Conformation and the sodium ion condensation on DNA and RNA structures in the presence of a neutral cosolute as a mimic of the intracellular media. Mol Biosyst. 2008; 4:579–588. [PubMed: 18493656]

24. Pincus DL, Hyeon C, Thirumalai D. Effects of trimethylamine N-oxide (TMAO) and crowding agents on the stability of RNA hairpins. J Am Chem Soc. 2008; 130:7364–7372. [PubMed: 18479134]

25. Muhuri S, Mimura K, Miyoshi D, Sugimoto N. Stabilization of three-way junctions of DNA under molecular crowding conditions. J Am Chem Soc. 2009; 131:9268–9280. [PubMed: 19566098]

26. Kilburn D, Roh JH, Guo L, Briber RM, Woodson SA. Molecular crowding stabilizes folded RNA structure by the excluded volume effect. J Am Chem Soc. 2010; 132:8690–8696. [PubMed: 20521820]

27. Lambert D, Leipply D, Draper DE. The osmolyte TMAO stabilizes native RNA tertiary structures in the absence of Mg2+: evidence for a large barrier to folding from phosphate dehydration. J Mol Biol. 2010; 404:138–157. [PubMed: 20875423]

28. Miller MC, Buscaglia R, Chaires JB, Lane AN, Trent JO. Hydration Is a Major Determinant of the G-Quadruplex Stability and Conformation of the Human Telomere 3' Sequence of d(AG(3)(TTAG(3))(3)). J Am Chem Soc. 2010
29. Zhang DH, Fujimoto T, Saxena S, Yu HQ, Miyoshi D, Sugimoto N. Monomorphic RNA G-quadruplex and polymorphic DNA G-quadruplex structures responding to cellular environmental factors. Biochemistry. 2010; 49:4554–4563. [PubMed: 20420470]
30. Knowles DB, Lacroix AS, Deines NF, Shkel I, Record MT Jr. Separation of preferential interaction and excluded volume effects on DNA duplex and hairpin stability. Proc Natl Acad Sci U S A. 2011
31. Inoko Y, Yamamoto M, Fujiwara S, Ueki T. X-ray scattering study of the shape of the DNA region in nucleosome core particle with synchrotron radiation. J Biochem. 1992; 111:310–316. [PubMed: 1587792]
32. Svergun DI, Koch MH, Serdyuk IN. Structural model of the 50 S subunit of Escherichia coli ribosomes from solution scattering. I. X-ray synchrotron radiation study. J Mol Biol. 1994; 240:66–77. [PubMed: 8021941]
33. Svergun DI, Pedersen JS, Serdyuk IN, Koch MH. Solution scattering from 50S ribosomal subunit resolves inconsistency between electron microscopic models. Proc Natl Acad Sci U S A. 1994; 91:11826–11830. [PubMed: 7991543]
34. Svergun DI, Koch MH, Pedersen JS, Serdyuk IN. Structural model of the 50S subunit of E. coli ribosomes from solution scattering. Basic Life Sci. 1996; 64:149–174. [PubMed: 9031510]
35. Qiu X, Kwok LW, Park HY, Lamb JS, Andresen K, Pollack L. Measuring inter-DNA potentials in solution. Phys Rev Lett. 2006; 96:138101. [PubMed: 16712040]
36. Qiu X, Andresen K, Kwok LW, Lamb JS, Park HY, Pollack L. Inter-DNA attraction mediated by divalent counterions. Phys Rev Lett. 2007; 99:038104. [PubMed: 17678334]
37. Andresen K, Qiu X, Pabit SA, Lamb JS, Park HY, Kwok LW, Pollack L. Mono- and trivalent ions around DNA: a small-angle scattering study of competition and interactions. Biophys J. 2008; 95:287–295. [PubMed: 18339743]
38. Pabit SA, Qiu X, Lamb JS, Li L, Meisburger SP, Pollack L. Both helix topology and counterion distribution contribute to the more effective charge screening in dsRNA compared with dsDNA. Nucleic Acids Res. 2009; 37:3887–3896. [PubMed: 19395592]
39. Pabit SA, Meisburger SP, Li L, Blose JM, Jones CD, Pollack L. Counting ions around DNA with anomalous small-angle X-ray scattering. J Am Chem Soc. 2010; 132:16334–16336. [PubMed: 21047071]
40. Tataurov AV, You Y, Owczarzy R. Predicting ultraviolet spectrum of single stranded and double stranded deoxyribonucleic acids. Biophys Chem. 2008; 133:66–70. [PubMed: 18201813]
41. Pollack L. SAXS Studies of Ion-Nucleic Acid Interactions. Annu Rev Biophys. 2011; 40:225–242. [PubMed: 21332357]
42. Pabit SA, Finkelstein KD, Pollack L. Using anomalous small angle X-ray scattering to probe the ion atmosphere around nucleic acids. Methods Enzymol. 2009; 469:391–410. [PubMed: 20946800]
43. McDowell JA, Turner DH. Investigation of the structural basis for thermodynamic stabilities of tandem GU mismatches: solution structure of (rGAGGUCUC)2 by two-dimensional NMR and simulated annealing. Biochemistry. 1996; 35:14077–14089. [PubMed: 8916893]
44. Li L, Pabit SA, Lamb JS, Park HY, Pollack L. Closing the lid on DNA end-to-end stacking interactions. Appl Phys Lett. 2008; 92:223901–2239013. [PubMed: 19488404]
45. Robinson, RA.; Storkes, RH. Electrolyte Solutions. Second Revised ed.. Dover Publications Inc.; Mineola, NY: 2002.
46. Stokes RH. Comparison of activity coefficients in the three-component system sodium chloride-sucrose-water from independent isopiestic and EMF measurements at 298.15 K. Journal of the Chemical Society, Faraday Transactions. 1995; 91:1457–1458.
47. Grilley D, Soto AM, Draper DE. Direct quantitation of Mg2+-RNA interactions by use of a fluorescent dye. Methods Enzymol. 2009; 455:71–94. [PubMed: 19289203]

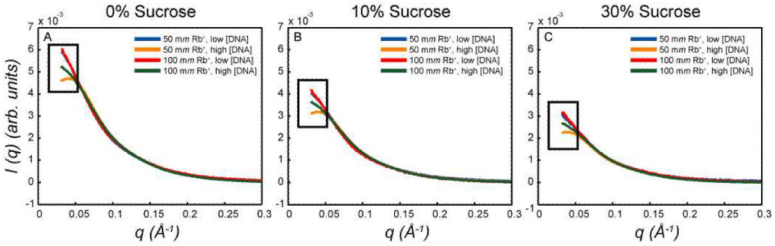


**Figure 1. Concentration Normalized Scattering Intensity Profiles of 25 bp Duplex DNA in $Rb^+$ acetate and Sucrose**

Panels A–C show *I(q)* vs. *q* for low and high DNA concentrations at 50 m*m* and 100 m*m* $Rb^+$ acetate with 0%, 10%, and 30% sucrose, respectively All curves shown are the average of 16–32 scattering images, with a standard deviation of approximately 1%. The overall decrease in signal from panel A to panel C is due to contrast variation effects of the sucrose. However, the same trends in the data are observed. The curves from the 50 m*m* $Rb^+$ samples fall below those from the 100 m*m* $Rb^+$ samples in the low *q* region consistent with greater repulsion in lower ionic strength. In addition, more repulsion is observed at higher DNA concentration, signaled by a more pronounced downturn in the intensity profile at low *q*.

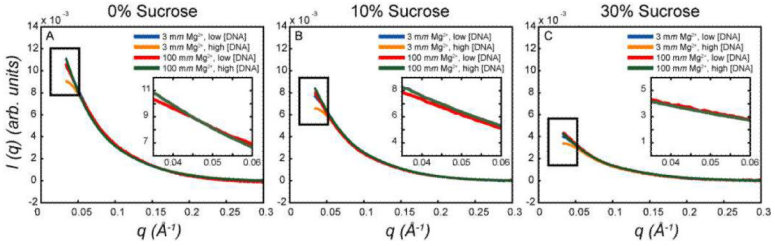


**Figure 2. Concentration Normalized Scattering Intensity Profiles of 25 bp Duplex DNA in $MgCl_2$ and Sucrose**

Panels A–C show *I(q)* vs. *q* for low and high DNA concentrations at 3 m*m* and 100 m*m* $MgCl_2$ with 0%, 10%, and 30% sucrose, respectively. All curves shown are the average of 16–32 scattering images, with a standard deviation of approximately 1%. The overall decrease in signal from panel A to panel C is due to contrast matching effects of the sucrose. Note that the same trends in the 3 m*m* $Mg^{2+}$ data are observed. The curves from the 3 m*m* $Mg^{2+}$ samples generally fall below those from the 100 m*m* $Mg^{2+}$ samples in the low *q* region consistent repulsion in 3 m*m* $Mg^{2+}$, and more repulsion is observed for the high DNA concentration samples in 3 m*m* $Mg^{2+}$ signaled by the downturn in the intensity profile at low *q* compared to the low concentration profiles. However, there is a difference in the 100 m*m* $Mg^{2+}$ samples with increasing sucrose. In no sucrose (A) the high concentration profile (green) falls above the low (red) concentration profile consistent with end-to-end stacking of the DNA duplexes. This difference is qualitatively less with increasing sucrose (B and C), suggesting less end-to-end stacking in sucrose. The insets are zoomed to $0.035 < q < 0.06$ to better show the change in trend at 100 m*m* $Mg^{2+}$ with increasing sucrose. .

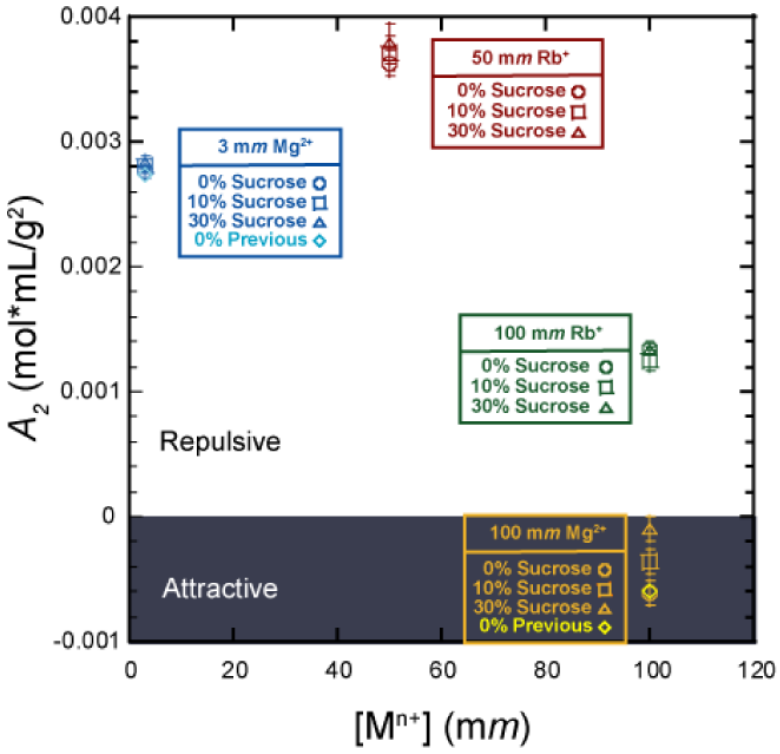


**Figure 3. $A_2$ vs. Monovalent or Divalent Cation Concentration**

Shows $A_2$ for 50 m*m* and 100 m*m* $Rb^+$ as well as 3 m*m* and 100 m*m* $Mg^{2+}$. For all of the repulsive conditions ($A_2 > 0$) the interaction potential among DNA duplexes remains unchanged within error with sucrose, and 0% sucrose data agrees with previously published values for the 3 m*m* $Mg^{2+}$ data.[38] The $A_2$ value for 100 m*m* $Mg^{2+}$ at 0% sucrose also agrees with previously published values[38], but the interaction potential decreases with increasing sucrose, suggesting disruption of end-to-end duplex stacking. Error bars shown are propagated from linear fits from Equations 2 or 3.

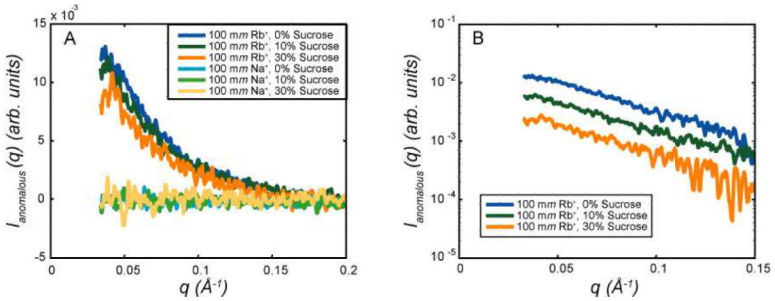


**Figure 4. Concentration Normalized ASAXS profiles for 100 m*m* $Rb^+$ acetate samples and 100 m*m* $Na^+$ acetate controls**

A) Shows ASAXS data for 0, 10, and 30% sucrose for $Rb^+$ and $Na^+$ controls The small differences in intensity may be from contrast matching effects of sucrose, and $Na^+$ controls show near zero anomalous scattering intensity. B) Shows the $Rb^+$ anomalous scattering intensity as in Panel A, but on a logarithmic scale (data offset by a multiplicative factor) to highlight the similarities in the shape of the curve decay with increasing sucrose. This shape similarity suggests the distribution of ions around the duplex is not changed by increasing sucrose concentration.

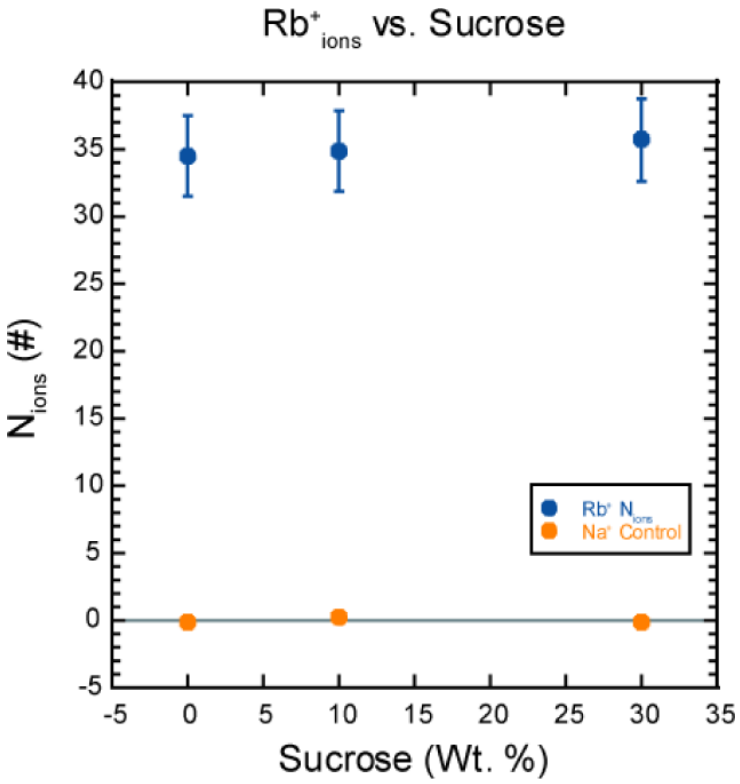


**Figure 5. $N_{ions}$ vs. Sucrose**

Shows $N_{ions}$ for $Rb^+$ and $Na^+$ controls at 0%, 10%, and 30% sucrose. Note that $N_{ions}$ is unchanged within error with increasing sucrose and agrees with previous results in 0% sucrose.[39] Controls are also unchanging with sucrose, and near zero since no resonant elements are present in the ASAXS measurement. Error bars shown are approximately 10% for both $Rb^+$ and $Na^+$ with the latter being small than the size of the data points.

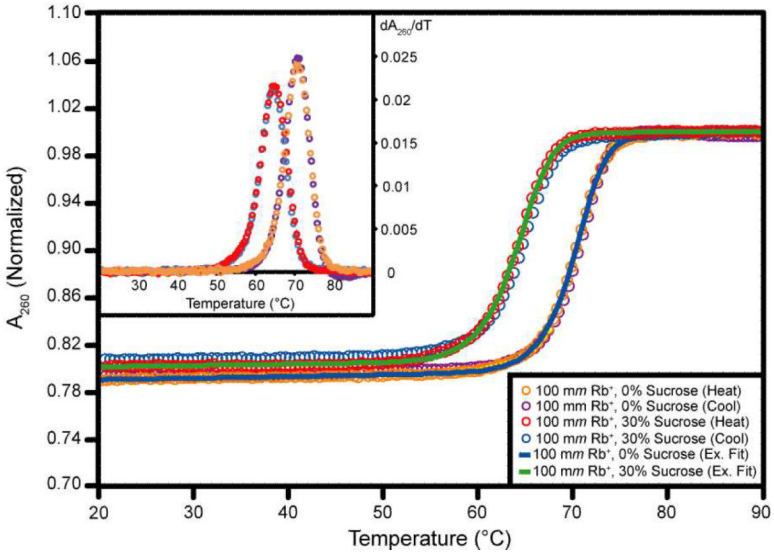


**Figure 6. Absorbance vs. Temperature Curves from Thermal Denaturations**

Shows representative heating and cooling melt curves for 100 m*m* $Rb^+$ data in 0% (orange, purple) and 30% (red, blue) sucrose. Curves have been corrected for buffer absorbance before fitting, and example fits from *Meltwin 3.5* are also shown for the heating curves. Fits of cooling data are similar, but omitted here for figure clarity. The inset shows the derivative of the melting curves with temperature. These data were smoothed using an 11-pt window.

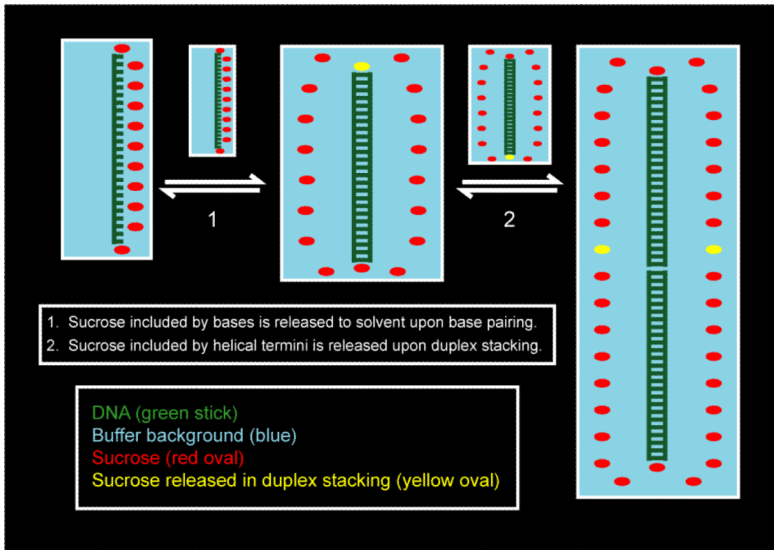


**Figure 7. Sucrose Influence on Folding and End-to-End Stacking in 25 bp DNA Duplexes**

Shown above in step one, sucrose accumulated by DNA bases in the single stranded state is released upon duplex formation. In step two, end-to-end stacking cause the release of sucrose included at the helix ends. With increasing sucrose this step is more unfavorable and less stacking is observed.

**Table 1**

Thermodynamic Parameters for Folding of 25 bp DNA Duplex

| *Samples* | $\Delta H°^{a}$ *(kcal/mol)* | $\Delta S°^{a}$ *(e.u.)* | $\Delta G°_{37}{}^{a}$ *(kcal/mol)* | $\Delta\Delta G°_{37}{}^{a}$ *(kcal/mol)* | $T_M{}^{a}$ *(°C)* | $\Delta T_M{}^{a}$ *(°C)* |
|---|---|---|---|---|---|---|
| 100 m*m* $Rb^+$ Acetate, 0% Sucrose | −201.3 ± 7.4 | −558 ± 22 | −28.14 ± 0.75 | - | 70.5 ± 0.4 | - |
| 100 m*m* $Rb^+$ Acetate, 30% Sucrose | −183.0 ± 5.9 | −516 ± 17 | −23.06 ± 0.53 | $5.08^{b}$ ± 0.91 | 64.5 ± 0.2 | $-6.0^{b}$ ± 0.4 |
| 50 m*m* $Rb^+$ Acetate, 0% Sucrose | −200.6 ± 8.2 | −563 ± 28 | −26.02 ± 0.49 | - | 65.8 ± 0.5 | - |
| 50 m*m* $Rb^+$ Acetate, 30% Sucrose | −179.1 ± 4.0 | −510 ± 12 | −20.75 ± 0.36 | $5.27^{c}$ ± 0.61 | 60.5 ± 0.6 | $-5.3^{c}$ ± 0.8 |
| 3 m*m* $MgCl_2$, 0% Sucrose | −214.2 ± 5.1 | −592 ± 15 | −30.60 ± 0.62 | - | 72.9 ± 0.2 | - |
| 3 m*m* $MgCl_2$, 30% Sucrose | −203.7 ± 9.4 | −569 ± 27 | −27.16 ± 1.14 | $3.44^{d}$ ± 1.30 | 68.3 ± 0.5 | $-4.6^{d}$ ± 0.5 |

[a]Errors are standard deviations of melting curves of at least two independent samples. An extra significant figure is included to eliminate rounding errors.

[b]Values are from comparison to 100 m*m* $Rb^+$ Acetate, 0% Sucrose

[c]Values are from comparison to 50 m*m* $Rb^+$ Acetate, 0% Sucrose

[d]Values are from comparison to 3 m*m* $MgCl_2$, 0% Sucrose